Volatility of methylglyoxal cloud SOA formed through OH radical oxidation and droplet evaporation

Diana L. Ortiz-Montalvo[1,3], Allison N. Schwier[2], Yong B. Lim[1,4], V.Faye McNeill[2], Barbara J. Turpin[5*]

[1]Environmental Sciences, Rutgers University, New Brunswick, NJ, USA

[2]Chemical Engineering, Columbia University, New York, NY, USA

[3]Current affiliation: National Institute of Standards and Technology, Gaithersburg, MD, USA

[4]Center for Environment, Health and Welfare Research, Korea Institute of Science and Technology, Seoul 02792, Republic of Korea

[5]Environmental Science and Engineering, University of North Carolina, Chapel Hill, NC, USA

*Corresponding author. Phone: (919) 966-3013; email: bjturpin@email.unc.edu

Abstract

The volatility of secondary organic aerosol (SOA) formed through cloud processing (aqueous hydroxyl radical (•OH) oxidation and droplet evaporation) of methylglyoxal (MGly) was studied. Effective vapor pressure and effective enthalpy of vaporization ($\Delta H_{vap,eff}$) were determined using 1) droplets containing MGly and its oxidation products, 2) a Vibrating Orifice Aerosol Generator (VOAG) system, and 3) Temperature Programmed Desorption Aerosol-Chemical Ionization Mass Spectrometry (TPD Aerosol-CIMS). Simulated in-cloud MGly oxidation (for 10-30 min) produces an organic mixture of higher and lower volatility components with an overall effective vapor pressure of $(4\pm7) \times 10^{-7}$ atm at pH 3. The effective vapor pressure decreases by a factor of 2 with addition of ammonium hydroxide (pH 7). The fraction of organic material remaining in the particle-phase after drying was smaller than for similar experiments with glycolaldehyde and glyoxal SOA. The $\Delta H_{vap,eff}$ of pyruvic acid and oxalic acid + methylglyoxal in the mixture (from TPD Aerosol-CIMS) were smaller than the theoretical enthalpies of the pure compounds and smaller than that

estimated for the entire precursor/product mix after droplet evaporation. After 10-30 min of aqueous oxidation (one cloud cycle) the majority of the MGly + $^{\bullet}$OH precursor/product mix (even neutralized) will volatilize during droplet evaporation; neutralization and at least 80 min of oxidation at 10^{-12} M $^{\bullet}$OH (or > 12 hr at 10^{-14} M) is needed before low volatility ammonium oxalate exceeds pyruvate.

1. Introduction

There is substantial evidence for secondary organic aerosol (SOA) formation through gas-phase oxidation followed by aqueous chemistry in clouds and wet aerosol (Blando and Turpin, 2000; Ervens et al., 2011; Herrmann et al., 2015). Organic compounds are predominantly emitted in the gas-phase (Fraser et al., 1996) where they are fragmented, oxidized and form small water-soluble organic compounds, which are ubiquitous and abundant in the atmosphere (Millet, 2005; Carlton and Turpin, 2013). The chemistry of several water-soluble organics (e.g., aldehydes, organic acids, ketones, phenols, epoxides) has been studied because of their potential to form SOA in the aqueous-phase (SOA_{aq}) by means of radical chemistry (e.g., hydroxyl radical reactions) and non-radical reactions (e.g., acid or ammonium catalyzed reactions) (e.g., Ervens et al., 2011; De Haan et al., 2011; McNeill, 2015). SOA_{aq} has also been observed to form through evaporation of droplets containing single organic compounds (e.g., glyoxal, methylglyoxal) that form oligomers through self-reactions (Loeffler et al., 2006; De Haan et al., 2009). The current study focuses on droplet evaporation of products formed by the OH-initiated oxidation of methylglyoxal (MGly) with hydroxyl radicals ($^{\bullet}$OH) in clouds (MGly SOA_{Cld}).

MGly ($C_3H_4O_2$) is a secondary gas-phase oxidation product of anthropogenic and biogenic hydrocarbons including isoprene (Atkinson and Arey, 2003; Seinfeld and Pandis, 2012; Fu et al., 2008). MGly is emitted by biomass burning (Hays et al., 2002), vehicles (Ban-Weiss et al., 2008) and from the sea surface (Lawson et al., 2015). Its gas-phase lifetime is 2 hr and 9 hr with respect to photolysis and $^{\bullet}$OH, respectively (Atkinson 2000). MGly is water soluble (effective Henry's law constant, $H_{eff} = 3.71 \times 10^3$ M atm^{-1} at 25°C) (Betterton and Hoffmann, 1988) and has been measured

58 in clouds (< 0.3-128 μM) (Munger et al., 1995). In the aqueous-phase, MGly reacts rapidly with •OH
59 (~26 min aqueous lifetime with respect to •OH) and forms several products found in the particle-
60 phase in the atmosphere (e.g., pyruvate, oxalate, and glyoxylate; Limbeck et al., 2001). At cloud
61 relevant concentrations, the reaction of MGly with •OH produces small carboxylic acids, mainly
62 pyruvic, acetic, and oxalic acids, and to a minor extent glyoxylic and glycolic acids (Tan et al.,
63 2010). In the highly concentrated solutions found in wet aerosols, non-radical (e.g., NH_4^+) reactions
64 become more important and radical reactions can form larger organic acids and oligomers (Lim et
65 al., 2013; McNeill, 2015). Additionally, MGly can form SOA_{aq} by self-oligomerization through aldol
66 condensation reactions in evaporating aqueous droplets (Loeffler et al., 2006; De Haan et al., 2009).
67 While SOA_{aq} formation is being added to chemical transport models (McNeill, 2015), a
68 better understanding of chemical transformations that occur during droplet evaporation (Loeffler et
69 al., 2006; De Haan et al., 2009; Ortiz-Montalvo et al., 2012, 2014) and the thermodynamic properties
70 of the SOA_{aq} mixture are needed to aid these efforts (Tsigaridis and Kanakidou, 2003). Michaud et
71 al. (2009) found that SOA_{aq} formed through aqueous OH oxidation of methacrolein and droplet
72 evaporation became less volatile with increasing oxidation (reaction time). Ortiz-Montalvo et al.
73 (2012) provided values of effective vapor pressure (~10^{-7} atm) and enthalpy of vaporization (~70
74 kJ/mol) for the precursor/product mixture formed through aqueous •OH oxidation (10-30 min) and
75 droplet evaporation of glycolaldehyde. They hypothesized that the vapor pressure of glycolaldehyde
76 SOA_{aq} would be orders of magnitude lower if the organic acid products (e.g. oxalate) were
77 neutralized to organic salts. Evidence to support this was provided by evaporating droplets of oxalic
78 acid and ammonium oxalate. More recently, Ortiz-Montalvo et al. (2014) verified that the volatility
79 of a glyoxal + •OH precursor/product mixture (after 10 min reaction) was significantly reduced when
80 the mixture was neutralized from pH 3 to pH 7 through the addition of ammonium hydroxide.
81 The present study provides, to our knowledge, the first reported estimates of the effective
82 vapor pressure ($p'_{L,eff.}$) and enthalpy of vaporization ($\Delta H_{vap,eff}$) of MGly cloud SOA_{aq} (SOA_{Cld})
83 formed through •OH oxidation and droplet evaporation in the presence (pH 7) and absence (pH 3) of
84 NH_4OH. This work seeks to better understand the gas-particle partitioning of SOA_{Cld}.

2. Methods

2.1 Overview

The purpose of this work is to characterize the volatility of SOA_{Cld} formed from in-cloud oxidation of MGly by OH radicals ($^{\bullet}OH$) followed by droplet evaporation. Vibrating Orifice Aerosol Generator (VOAG) and Temperature Programmed Desorption Aerosol Chemical Ionization Mass Spectrometry (TPD Aerosol-CIMS) systems were used to determine $p'_{L,eff.}$ and $\Delta H_{vap,eff}$ of the MGly + $^{\bullet}OH$ precursor/product mix in evaporating droplets for two different atmospheric scenarios. The aqueous chemistry of MGly and $^{\bullet}OH$ has previously been validated by comparing predicted and measured precursor/product concentration dynamics in laboratory batch reactor experiments (Tan et al., 2010; Lim et al., 2013). We used this chemistry to determine the precursor/product compositional mix resulting from the $^{\bullet}OH$ oxidation (10^{-12} M) of 5 μM MGly in cloud droplets (10-30 min) using 1) a batch reactor and 2) a continuously stirred tank reactor (CSTR) approximation. Mimic solutions prepared with these compositions were used in droplet evaporation experiments. The VOAG system provided information about the volatility behavior of the mixture, whereas the TPD Aerosol-CIMS characterized the behavior of individual species within the mixture.

2.2 Chemical Modeling

Previously published chemical models were used (Tan et al., 2010; Lim et al., 2013). In batch reactor modeling (Tan et al., 2010), the initial MGly concentration was 5 μM, within the concentration range found in cloud water (Munger et al., 1995). This corresponds to a gas-phase MGly concentration of ~1 ppb, given a Henry's law constant of H= 3.71×10^3 M atm^{-1} (Betterton and Hoffmann, 1988). MGly decreased as the reaction proceeded. The concentration of $^{\bullet}OH$ was held constant at 10^{-12} M, an upper bound for cloud water (Ervens et al., 2014). For CSTR modeling (Lim et al., 2013), the aqueous MGly concentration was maintained always at 5 μM and the $^{\bullet}OH$ concentration at 10^{-12} M. Note, modeled composition at 10^{-13} and 10^{-14} M OH are provided in Fig. S1.

MGly is formed in the atmosphere from many precursor gases; thus it is not immediately apparent whether the batch reactor or CSTR approximation is more appropriate for modeling the

chemical composition. If gas-phase production of MGly is slow relative to its aqueous oxidation, a batch reactor may be a better approximation. If, on the other hand, gas-phase MGly production (and aqueous uptake) is rapid relative to aqueous oxidation, MGly will continue to be replenished in the aqueous-phase as oxidation takes place, and the aqueous oxidation system will be better represented as a CSTR. However, you will find below that effective vapor pressures determined for both Batch and CSTR assumptions were similar. This chemistry is likely to be oxidant (rather than MGly) limited (Ervens et al., 2014).

2.3 Mimic Samples

Mimic solutions were prepared to match the chemical composition 10-30 minutes into batch and CSTR reactions. Concentrations of species were scaled up 13-130 times for CSTR, and 25-250 times for batch) creating 6 concentrations from approximately 500-4000 μM-C all above the detection limits of the droplet evaporation system, while maintaining the same distribution of species. Thus, droplet evaporation experiments were conducted with solutions that were initially more concentrated than typical cloud droplets and as a result, experiments do not include any chemistry that occurs at the initial (most dilute) stage of droplet evaporation. Mimics were prepared using 18 MΩ milli-Q water, methylglyoxal (37.8%; Sigma-Aldrich) and pyruvic (99.1%; Sigma-Aldrich), oxalic (0.1008 N; Fluka Analytical), and acetic (99.99%; Sigma-Aldrich) acids. To study the effects of increasing pH, we added ammonium hydroxide (29.6% as ammonia (NH_3); J.T. Baker) to selected CSTR mimics.

2.4 VOAG Droplet Evaporation Experiments

Monodisperse droplets (droplet diameter, D_d = 17.9±0.4 μm, n=3, r^2=0.99) of mimic samples were generated and evaporated using a VOAG (TSI Model 3450; Berglund and Liu, 1973) followed by a dilution drying chamber (residence time 6 s, 12±3% RH, 24.1±0.4 ºC). The diameter of the resulting particles (e.g., SOA) was measured with an optical particle counter (OPC) downstream of an ionizer, as described previously (Ortiz-Montalvo et al., 2012) and in Supplemental Information.

The volatility of SOA_{Cld} was assessed as described previously (Ortiz-Montalvo et al., 2012). Briefly, six dilutions (0 - 4000 μM C) of each mimic solution and organic standard (acetic, oxalic, succinic, glutaric, and tartaric acids) were passed through the VOAG. Resulting droplets were dried to ~10% RH; their dry diameter was measured in the OPC and the mass of residual particles (*PM mass*) was calculated using assumptions given in Table S1). In addition, each mimic solution was analyzed for total organic carbon (TOC) and converted to organic matter (OM mass). The *PM mass* of the organic standards was regressed on *OM mass,* and the slopes of each were evaluated against their corresponding liquid vapor pressures ($p°_L$) (SIMPOL group contribution method; Pankow and Asher, 2008) and enthalpies of vaporization (ΔH_{vap}) (Joback and Reid, 1987; group contribution method using normal boiling points to estimate ΔH_{vap} of pure compounds). Sigmoidal fits were obtained since the *PM mass* divided by droplet *OM mass* (*PM mass / OM mass*$_{(droplet)}$) reflects the particle fraction (i.e., fraction of the total droplet organic matter that remained in the particle-phase). Because some organic compounds, like tartaric acid, retain water even at 5% RH (Peng et al., 2001), a correction was made to the original sigmoidal curve to account for the effect of residual water on particle density, as described previously (Ortiz-Montalvo et al., 2012). The $p'_{L,eff}$ and $\Delta H_{vap,eff}$ of the mimics (mix of MGly precursors and products) were estimated from the corrected sigmoidal curves. The estimated $p'_{L,eff.}$ for malonic acid ($1\pm1 \times 10^{-7}$ atm), analyzed as an independent check (6 dilutions between 0-3000 μM C from 0.999 %, Sigma-Aldrich), is of the same order of magnitude as the calculated theoretical value ($2\pm2 \times 10^{-7}$ atm) (Pankow and Asher, 2008). The estimated $\Delta H_{vap,eff.}$ (72±2 kJ/mol) differed from the theoretical value by 4% (69.12 ± 1.79 kJ/mol) (Joback and Reid, 1987). A ~17% uncertainty is introduced because of differences in refractive index of malonic acid (1.479) and polystyrene latex particles (1.59; used for OPC manufacturer-supplied calibration).

Droplet evaporation experiments were also run with 1 mM standards: oxalic acid, oxalic acid + ammonium hydroxide, ammonium oxalate (99.0%; Fluka Analytical), pyruvic acid, pyruvic acid + ammonium hydroxide, and sodium pyruvate (100 mM; Thermo Scientific) (Fig. 1). Ammonium hydroxide, when used, was added to adjust the solution to pH 7. The ratio of the residual PM volume

to $OM\ mass_{(droplet)}$ ($PM\ vol.\ /\ OM\ mass_{(droplet)}$) for oxalic acid + ammonium hydroxide was identical to that of ammonium oxalate, verifying that the addition of ammonium hydroxide effectively neutralized organic acids (Fig. 1). Note that $PM\ vol.\ /\ OM\ mass_{(droplet)}$ is proportional to the fraction remaining in the particle-phase and increases with decreasing vapor pressure. In addition, neutralization of oxalic acid (ammonium oxalate production) had a larger effect on $PM\ vol.\ /\ OM\ mass_{(droplet)}$ than pyruvic acid neutralization (Fig. 1), presumably because ammonium oxalate has a lower vapor pressure (Paciga et al., 2014).

2.5 TPD Aerosol-CIMS Analysis

Bulk mimic solutions were also analyzed by TPD Aerosol-CIMS, as described previously (Ortiz-Montalvo et al., 2014; Drozd et al., 2014; Hakkinen et al., 2014; McNeill et al., 2007). Briefly, bulk mimic solutions were aerosolized, dried and combined with a dry N_2 dilution flow (3.5-9.5 L/min) to ~12% RH. The aerosol had a lognormal number size distribution with a geometric mean particle diameter of 29±3 nm and geometric standard deviation of 1.3 (measured by scanning mobility particle sizer after drying). Organics were then volatilized at 25-116ºC for gas-phase detection by CIMS (McNeill et al., 2007; Ortiz-Montalvo et al., 2014). The residence time from atomization to CIMS detection was ~6 seconds. CIMS measurements were made in negative mode using I^- reagent ions.

MGly and oxalic, pyruvic and acetic acids are detectable in the negative mode. Oxalic acid and MGly both appear at *m/z* 217 as $I^-\cdot C_2H_2O_4$ and $I^-\cdot C_3H_4O_2\cdot H_2O$, respectively. Pyruvic acid appears at *m/z* 215 as $I^-\cdot C_3H_4O_3$. Acetic acid is detected at *m/z* 187 as $I^-\cdot C_2H_4O_2$; however, no analysis of acetic acid was performed because initial evaluations showed a constant signal over the range of temperature tested, suggesting it was present entirely in the gas-phase at 25ºC. The Clausius-Clapeyron relation was used to calculate the $\Delta H_{vap,eff.}$ (kJ/mol) for individual species present in the mixture (Ortiz-Montalvo et al., 2014).

Each mimic solution was analyzed at least twice. A solution of 1 mM oxalic acid standard (from 0.05 M; Fluka Analytical) was also analyzed (only once); its measured $\Delta H_{vap,eff.}$ (69±33

kJ/mol) was within 22-29% of the theoretical value (91-101 kJ/mol; Yaws, 2003) for the temperature range used (25-37ºC).

3. Results

3.1 Modeled Droplet Composition

Precursor and product concentration dynamics as well as composition of mimics at 10 and 30 minutes are shown (Fig. 2) because these are typical cloud droplet life times (Desboeufs et al., 2003; Ervens and Volkamer, 2010). Among the four mimics, the 30 min Batch and 10 min CSTR mimic samples were the most different. Therefore, we selected these for droplet evaporation experiments, in order to bound the range of $p'_{L,eff.}$ and $\Delta H_{vap,eff.}$ of the precursor/product mixtures formed after one cloud processing cycle of MGly in the presence of $^{\bullet}$OH. (Note, an air mass encountering cloudy conditions typically undergoes multiple (~10) cloud cycles of 10-30 min duration over the course of a day (Ervens and Volkamer, 2010).) The continuous accumulation of pyruvic acid (pink line) observed in the CSTR model is due to the continuous dissolution of gas-phase MGly in the CSTR model. Formaldehyde mainly forms from the reaction of $^{\bullet}$OH and acetic acid (a major product of MGly + $^{\bullet}$OH) (Tan et al., 2012; Lim et al., 2013).

3.2 VOAG – Vapor Pressure and Enthalpy of Vaporization

The $p'_{L,eff.}$ and $\Delta H_{vap,eff.}$ of CSTR and Batch mimics were comparable: 3-6 × 10^{-7} atm and 67-69 kJ/mol, respectively (Table 1, Figs. 3 and S1). The 30 min Batch mimic, which had a higher percentage of organic acids and less MGly, had a slightly lower but not significantly different $p'_{L,eff}$ than the 10 min CSTR mimic (p = 0.01, t-test, two-tailed). Similarly, the reduction in $p'_{L,eff}$ accomplished by neutralization (pH 7) of the CSTR mimic was small (factor of two) and the difference was not significant (p = 0.01, t-test, two-tailed).

Fig. 3 shows the residual particle mass (*PM mass*) and mass of organic matter in the droplet ($OM\ mass_{(droplet)}$) from droplet evaporation experiments conducted with organic acid standards and mimics. The *PM mass* of organic acid standards (oxalic, succinic, glutaric, and tartaric acids) is well correlated with $OM\ mass_{(droplet)}$ (r^2 = 0.84-0.99) with the exception of acetic acid, which is volatile.

215 The slopes (*PM mass / OM mass*$_{(droplet)}$) reflect the fraction of total droplet organic matter remaining
216 in the particle-phase (e.g., particle fraction) and are reported in Table 1 with coefficients of
217 determination (r^2) of *PM mass* on *OM mass*$_{(droplet)}$ for Batch 30 min (solid blue circles) and CSTR 10
218 min (at pH 3 and pH 7; solid black triangles and red squares, respectively). SOA yields are reported
219 in Section S3. The sample with the highest particle fraction was the neutralized (pH 7) 10 min CSTR
220 mimic. In contrast, the sample with the lowest particle fraction was the 10 min pH 3 CSTR mimic.
221 The sigmoidal curve in the inset of Fig. 3 is a fit to the *PM mass / OM mass*$_{(droplet)}$ versus log
222 p°_{L} for the organic acid standards, uncorrected (dashed) and corrected (solid) for the upper bound
223 influence of retained water on density. Also shown in the inset are the corresponding *PM mass / OM*
224 *mass*$_{(droplet)}$ values for the Batch (inset middle blue dashed arrow) and CSTR samples (inset upper red
225 arrow for pH 7; lower green dashed arrow for pH 3), pointing to their corresponding estimated $p'_{L,eff}$.
226 The $p'_{L,eff}$ values, taken from the sigmoidal regression, are reported in Table 1. Overall, the
227 volatilities of the three mimics were within a factor of two, with the largest difference found between
228 the 10 min CSTR mimic at pH 7 (3×10^{-7} atm) and pH 3 (6×10^{-7} atm). There was a factor of two
229 decrease in volatility with increasing pH. A decrease in volatility with addition of ammonium is
230 consistent with lower reported vapor pressures of organic acid salts compared to their corresponding
231 acids (Fig. 1). The decrease is modest presumably because of the modest effect of ammonia addition
232 on pyruvic acid (compared to the much larger effect of ammonia addition on oxalic acid).
233 Values of $\Delta H_{vap,eff.}$ for Batch and CSTR mimics (Table 1) were estimated using a similar
234 approach (Fig. S2). $\Delta H_{vap,eff}$ estimates (~68 kJ/mol) for the mix of MGly + $^{\bullet}$OH precursors and
235 products (mimics) fall within the range of the ΔH_{vap} values of the pure individual components that
236 comprised the CSTR and Batch samples (23-73 kJ/mol, at normal boiling point; Yaws 2003). No
237 significant difference was observed between $\Delta H_{vap,eff}$ estimates for the different mimics. A difference
238 of ~40-50% is observed between theoretical (molar-weighted enthalpies) and effective ΔH_{vap} (Table
239 1). Possible reasons are discussed below.

This work suggests that the MGly + •OH precursor/product mix created after processing through one cloud cycle (10-30 min) has a $p'_{L,eff}$ and $\Delta H_{vap,eff.}$ of (4±7) × 10^{-7} atm and 68±3 kJ/mol, respectively. Note that longer in-cloud reaction times (i.e., multiple cloud cycles) will push the product mix toward oxalate, which if present as a salt would lower the volatility of the mixture substantially (see ammonium oxalate slopes, Fig.1). Ammonium oxalate has a vapor pressure of ~10^{-11} atm (U.S. EPA 2010).

3.3 TPD Aerosol-CIMS – Enthalpy of Vaporization of Methylglyoxal Mimics

$\Delta H_{vap,eff.}$ of selected individual organic aerosol species formed from the CSTR and Batch mixtures and estimated by TPD Aerosol-CIMS are given in Table 2. While oligomers might have formed during the atomization and drying processes, their evolution was not observed at the temperatures used. $\Delta H_{vap,eff}$ values for pyruvic acid (*m/z* 215) and oxalic acid + methylglyoxal (*m/z* 217) were both lower than the theoretical ΔH_{vap} values of the pure compounds. For example, the $\Delta H_{vap,eff}$ of pyruvic acid in the mixture was ~5-19 kJ/mol compared to the theoretical ΔH_{vap} of pure pyruvic acid (48-52 kJ/mol) in the temperature range of 25-116ºC (Yaws 2003). The reduction in $\Delta H_{vap,eff}$ for a compound in a mixture compare to the ΔH_{vap} of the pure compound is consistent with previous findings by Ortiz-Montalvo et al. (2014), McNeill et al. (2007) and Donahue et al. (2005). Changes in $\Delta H_{vap,eff}$ with pH are within the measurement uncertainty (Table 2). TPD Aerosol-CIMS supporting data can be found in Section S2 of Supplemental Information; these results are discussed in further detail below.

4. Discussion and Conclusions

In this study, effective enthalpies of vaporization were measured for mimics of the MGly + •OH precursor/product mixtures present after one cycle (10-30 min) of simulated cloud processing (68±3 kJ/mol; VOAG) and for selected individual compounds in aerosols generated from the mixture (5-19 kJ/mol pyruvic acid, 31-34 kJ/mol MGly + oxalic acid; TPD Aerosol-CIMS). The VOAG system also measured $p'_{L,eff.}$ of the MGly + •OH precursor/product mixture, (4±7) × 10^{7} atm, which

decreased by only a factor of two with neutralization from pH 3 to 7 (i.e., through addition of ammonium hydroxide).

The $\Delta H_{vap,eff.}$ of the MGly + •OH precursor/product mixture (VOAG system) was similar (Table S2) to that measured for the precursor/product mix from glycolaldehyde + •OH (~70 kJ/mol) and glyoxal + •OH (~70 kJ/mol) using the same approach (Ortiz-Montalvo et al., 2012; 2014). VOAG results fell within the range of ΔH_{vap} values for the pure individual components in the mixtures. The observed difference (~40-50%) between theoretical (molar-weighted) and VOAG-estimated enthalpies reported here (Table 1) could be due to (1) compounds formed during droplet evaporation (e.g., methylglyoxal oligomers, imidazoles) that were not included in the theoretical calculation, and/or (2) retention of residual water in the measurements of the VOAG, which would result in larger measured diameters (thus PM volume and mass) and consequently larger *PM mass / OM mass*$_{(droplet)}$ ratios and higher VOAG enthalpy estimates. Based on this assessment the values we report in Table 1 are likely to be upper-bound estimates. In contrast to the VOAG results for $\Delta H_{vap,eff.}$ of precursor/product mixtures, the (TPD Aerosol-CIMS) $\Delta H_{vap,eff.}$ of individual compounds within the mimic aerosols were smaller than the $\Delta H_{vap,eff.}$ values of the pure compounds, in agreement with other TPD Aerosol-CIMS measurements of the ΔH_{vap} of individual species within internally mixed aerosol particles.

The $\Delta H_{vap,eff.}$ values obtained by the VOAG method for the MGly + •OH mimic mixtures are much larger than those obtained for pyruvic acid and oxalic acid + MGly from the TPD Aerosol-CIMS method. This is not surprising since the TPD Aerosol-CIMS tracks the evolution of individual organic components from the aerosols, whereas in the VOAG experiments *PM mass/OM mass*$_{(droplet)}$ values reflect the fraction of the *total* mimic organic matter that remains in the particle-phase. This quantity is compared to *PM mass / OM mass*$_{(droplet)}$ values for single standards of known $\Delta H_{vap,eff}$. So the results reflect the $\Delta H_{vap,eff}$ of the entire mimic mixture and any products formed during the evaporation process (e.g., oligomers). For example, MGly is among the components of this mixture. A portion of MGly will evaporate and a portion is likely to oligomerize during droplet evaporation. In either case it will influence the $\Delta H_{vap,eff}$ of the mixture as measured in the VOAG. On the other

hand, in the TPD Aerosol-CIMS, the $\Delta H_{vap,eff}$ values of MGly oligomers were not measured because they do not volatilize at the temperatures used in our experiments ($\leq$ 116°C).

The $p'_{L,eff}$ of the CSTR and Batch methylglyoxal + •OH precursor/product mimic mixtures are very similar to the $p'_{L,eff}$ (1-2 × 10^{-7} atm) measured for the mixture produced from the OH-initiated oxidation of (1 mM) glycolaldehyde with (~10^{-12} M) •OH in a batch reactor using the same VOAG system (Ortiz-Montalvo et al., 2012). In the glycolaldehyde study, we argued that the $p'_{L,eff}$ would be orders of magnitude lower if the organic acids were neutralized (pH 7) since organic salts have much lower vapor pressures than the organic acids. We still believe that this is true for glycolaldehyde because oxalate is a major oxidation product, at least at 40 min, and the volatility of ammonium oxalate is 4 orders of magnitude lower than that of oxalic acid (Fig. 1). Additionally, the fact that oxalic acid is found in the atmosphere predominantly in the particle-phase (Limbeck et al., 2001), despite its high vapor pressure, suggests that it is present in the atmosphere in a lower volatility form (e.g., a salt or complex). Furthermore, in our glyoxal study we found that neutralization did in fact reduce the volatility of aqueous glyoxal + •OH mixture (Ortiz-Montalvo et al., 2014). However, in the current MGly study, the addition of ammonia (from pH 3 to 7) to the CSTR 10 min sample (i.e. to form ammonium pyruvate) lowered the $p'_{L,eff.}$ by only a factor of 2 and not orders of magnitude as we expected. The degree of vapor pressure reduction is likely to depend on the properties of the organic salts being formed as seen in Fig. 1. In Fig. 1, values of PM volume/OM mass (from the VOAG System) and sub-cooled liquid vapor pressures are provided for pyruvic and oxalic acids and their ammonium and/or sodium salts. Clearly, ammonium salt formation reduces the vapor pressure of pyruvate, but not to the degree observed for oxalate. Nevertheless, atmospheric measurements have found that most pyruvate is in the particle-phase (e.g., 61%) (Limbeck et al., 2001). These results and our previous findings indicate that organic salt formation can play an important role in the properties and fate of SOA formed through cloud processing, but that it will depend on the gas-particle partitioning of the formed salts. There is a need to better understand the predominant forms that these organic acids take in the atmosphere because of their effect on gas-particle partitioning of SOA.

While this work produced a mix of lower and higher volatility products with an intermediate volatility (3×10^{-7} atm in the presence of ammonia), there are several ways in which the volatility of MGly SOA_{Cld} mix might decrease further. 1) Because of its high oxygen-to-carbon ratio (O:C ~ 0.8-1.1), we expect this material to re-dissolve and undergo additional cloud processing cycles. Based on our model results we expect oxalate to exceed pyruvate after 10-20 cloud cycles (one or two days) given 10^{-12} M OH (Fig. S3). Note that ammonium oxalate has a vapor pressure of ~10^{-11} atm (Paciga et al, 2014; Fig. 1). Thus we expect 1-2 days of cloud processing to lead to a substantial reduction in the volatility of the MGly + •OH precursor/product mix. However if the aqueous OH concentration is 10^{-13} or 10^{-14} M, 20 to more than 70 cycles (a day to in excess of a week) of cloud processing would be required before oxalate dominates. Concentrations of OH radicals in clouds are not well constrained due to an incomplete understanding of aqueous-phase OH production and loss, especially involving organics. 2) Aqueous chemistry can also continue in the wet aerosol that is present in the cloud outflow. The much higher concentrations in wet aerosols alter the chemistry and promote oligomer formation through radical and non-radical reactions (DeHaan et al., 2011; Lim et al., 2013). 3) The predominant chemical form of the organic acid products of MGly + •OH (pyruvate, oxalate, acetate) in the atmosphere is not known. Binding with other cations (e.g. to form other salts) or with transition metals (Weller et al., 2014) could potentially reduce the volatility of this mix. This could occur via acid displacement reactions (e.g., Laskin et al., 2012) or reactions with polyvalent metal ions (e.g., Furukawa and Takahashi, 2011).

In conclusion, effective vapor pressure ($p'_{L,eff.}$) and enthalpy of vaporization ($\Delta H_{vap,eff.}$) values were estimated for the aqueous oxidation products of methylglyoxal with •OH (as modeled at cloud relevant conditions using two atmospheric scenarios) followed by droplet evaporation (MGly SOA_{Cld}). The volatility assessment indicated that neutralization of MGly + •OH organic acid products with ammonia resulted in only a modest (not statistically significant) decrease in the $p'_{L,eff.}$ (3-6 × 10^{-7} atm) and increase in the $\Delta H_{vap,eff.}$ (67-69 kJ/mol). The volatility of MGly SOA_{Cld} was also comparable between the Batch (MGly depletion) and CSTR (MGly at steady-state) models. Our study shows that for one cloud cycle the MGly + •OH precursor/product mix (even neutralized) has

346 an intermediate vapor pressure, meaning that a majority of this organic mixture will not remain in a
347 dry particle after droplet evaporation. There are several ways that the fraction found in the particle-
348 phase might be greater (lower volatility): (1) pyruvate (main product) could be present in a different
349 chemical form, (2) chemical processing could take place for multiple cloud cycles (one to several
350 days) to reach a maximum yield of oxalate, (3) chemical processing could continue in the wet
351 aerosol formed after droplet evaporation forming low-volatility oligomers, (4) water bound to the
352 hygroscopic particle could enhance retention of the soluble, intermediate volatility products. The
353 gas-particle partitioning of atmospheric pyruvate remains uncertain and affects our understanding of
354 methylglyoxal as a SOA_{Cld} precursor.

355 **5. Acknowledgements**

356 This research was supported, in part, by a Ford Foundation Dissertation Fellowship Award;
357 Air Pollution Educational and Research Grant, Mid-Atlantic States Section of Air and Waste
358 Management Association; Department of Education, Graduate Assistance in Areas of National Need
359 (P200A060156); National Science Foundation (ATM-0630298), National Oceanic and Atmospheric
360 Association (NA07OAR4310279), US Environmental Protection Agency Science To Achieve
361 Results (RD-83375101-0), New Jersey Agricultural Experiment Station; USDA-NIFA. VFM and
362 ANS acknowledge support of NASA Tropospheric Chemistry (NNX09AF26G). This research was
363 not subjected to government agency review. It does not necessarily reflect views of any government
364 agency. No official endorsement should be inferred.

365 **6. References**

366 Atkinson, R., 2000. Atmospheric chemistry of VOCs and NOx. Atmos. Environ. 34, 2063-2101.
367 Atkinson, R., Arey, J., 2003. Atmospheric degradation of volatile organic compounds. Chem. Rev.
368 103, 4605-4638.
369 Ban-Weiss, G. A., McLaughlin, J. P., Harley, R. A., Kean, A. J., Grosjean, E., Grosjean, D. 2008.
370 Carbonyl and nitrogen dioxide emissions from gasoline-and diesel-powered motor vehicles.
371 *Environ. Sci. Technol.*, *42*, 3944-3950.
372 Berglund, R.N., Liu, B.Y.H., 1973. Generation of monodisperse aerosol standards. Environ. Sci.
373 Technol. 7, 147-153.
374 Betterton, E.A., Hoffmann, M.R., 1988. Henry's law constants of some environmentally important
375 aldehydes. Environ. Sci. Technol. 22, 1415-1418.
376 Blando, J.D., Turpin, B.J., 2000. Secondary organic aerosol formation in cloud and fog droplets: a
377 literature evaluation of plausibility. Atmos. Environ. 34, 1623-1632.
378 Carlton, A.M., Turpin, B.J. (2013) Particle partitioning potential of organic compounds is highest in

379 the eastern US and driven by anthropogenic water, *Atmos. Phys. Chem.,* 13, 10203-10214.
380 Chickos, J.S., Zhao, H., 2005. Measurement of the vaporization enthalpy of complex mixtures by
381 correlation-gas chromatography. The vaporization enthalpy of RP-1, JP-7, and JP-8 rocket
382 and jet fuels at T= 298.15 K. Energy Fuels 19, 2064-2073.
383 De Haan, D.O., Corrigan, A.L., Tolbert, M.A., Jimenez, J.L., Wood, S.E., Turley, J.J., 2009.
384 Secondary organic aerosol formation by self-reactions of methylglyoxal and glyoxal in
385 evaporating droplets. Environ. Sci. Technol. 43, 8184-8190.
386 De Haan, D.O., Hawkins, L.N., Kononenko, J.A., Turley, J.J., Corrigan, A.L., Tolbert, M.A.,
387 Jimenez, J.L., 2011. Formation of nitrogen-containing oligomers by methylglyoxal and
388 amines in simulated evaporating cloud droplets. Environ. Sci. Technol. 45, 984-991.
389 Desboeufs, K., Losno, R., Colin, J., 2003. Relationship between droplet pH and aerosol dissolution
390 kinetics: Effect of incorporated aerosol particles on droplet pH during cloud processing. J
391 Atmos. Chem. 46, 159-172.
392 Donahue, N.M., Huff Hartz, K.E., Chuong, B., Presto, A.A., Stanier, C.O., Rosenhørn, T., Robinson,
393 A.L., Pandis, S.N., 2005. Critical factors determining the variation in SOA yields from
394 terpene ozonolysis: A combined experimental and computational study. Faraday Discuss.
395 130, 295-309.
396 Drozd, G.T., Woo, J.L., Hakkinen, S.A.K., Nenes, A., McNeill, V.F., 2014. Inorganic salts interact
397 with organic di-acids in submicron particles to form material with low hygroscopicity and
398 volatility. *Atmos. Chem. Phys.,* 14, 5205-5215.
399 Ervens, B., Volkamer, R., 2010. Glyoxal processing by aerosol multiphase chemistry: towards a
400 kinetic modeling framework of secondary organic aerosol formation in aqueous particles.
401 Atmos. Chem. Phys. 10, 8219-8244.
402 Ervens, B., Turpin, B.J., Weber, R.J., 2011. Secondary organic aerosol formation in cloud droplets
403 and aqueous particles (aqSOA): a review of laboratory, field and model studies. Atmos.
404 Chem. Phys. 11, 11069-11102.
405 Ervens, B., Lim, Y.B., Sorooshian, A., Turpin, B.J., 2014. Key parameters controlling aqSOA
406 formation. J. Geophys. Res. 119, 3997-4016.
407 Fraser, M.P., Grosjean, D., Grosjean, E., Rasmussen, R.A., Cass, G.R., 1996. Air quality model
408 evaluation data for organics. 1. Bulk chemical composition and gas/particle distribution
409 factors. Environ. Sci. Technol. 30, 1731-1743.
410 Fu, T.M., Jacob, D.J., Wittrock, F., Burrows, J.P., Vrekoussis, M., Henze, D.K. 2008. Global
411 budgets of atmospheric glyoxal and methylglyoxal, and implications for formation of
412 secondary organic aerosols. *J. Geophys. Res. Atmos. 113*(D15) doi:10.1029/2007JD009505.
413 Furukawa, T., Takahashi, Y., 2011. Oxalate metal complexes in aerosol particles: implications for
414 the hygroscopicity of oxalate-containing particles. Atmos. Chem. Phys. 11, 4289–4301.
415 Hakkinen, S.A.K., McNeill, V.F., Riipinen, I.A., 2014. Effect of Inorganic Salts on the Volatility of
416 Organic Acids *Environ. Sci. Technol., 48* 13718-13726.
417 Hays, M.D., Geron, C.D., Linna, K.J., Smith, N.D., Schauer, J.J., 2002. Speciation of gas-phase and
418 fine particle emissions from burning of foliar fuels. Environ. Sci. Technol. 36, 2281-2295.
419 Herrmann, H., Schaefer, T., Tilgner, A., Styler, S.A., Weller, C., Teich, M., Otto, T., 2015.
420 Tropospheric aqueous-phase chemistry: Kinetics, mechanisms, and its coupling to a changing
421 gas phase. Chemical Reviews. Article ASAP. DOI: 10.1021/cr500447k
422 Hilal, S.H., Karickhoff, S.W., Carreira, L.A., 2003. Prediction of the vapor pressure boiling point,
423 heat of vaporization and diffusion coefficient of organic compounds. QSAR Comb. Sci. 22,
424 565-574.
425 Joback, K.G., Reid, R.C., 1987. Estimation of pure-component properties from group-contributions.
426 Chem. Eng. Comm. 57, 233-243.
427 Laskin, A., Moffet, R.C., Gilles, M.K., Fast, J.D., Zaveri, R.A., Wang, B., Nigge, P., Shutthanandan,
428 J., 2012. Tropospheric chemistry of internally mixed sea salt and organic particles: Surprising
429 reactivity of NaCl with weak organic acids. J. Geophys. Res. 117, D15302.

Lawson, S. J., Selleck, P. W., Galbally, I. E., Keywood, M. D., Harvey, M. J., Lerot, C., Helmig, D., Ristovski, Z., 2015. Seasonal in situ observations of glyoxal and methylglyoxal over the temperate oceans of the Southern Hemisphere. *Atmos. Chem. Phys.* 15, 223-240.

Limbeck, A., Puxbaum, H., Otter, L., Scholes, M.C., 2001. Semivolatile behavior of dicarboxylic acids and other polar organic species at a rural background site (Nylsvley, RSA). Atmos. Environ. 35, 1853-1862.

Lim, Y.B., Tan, Y., Turpin, B.J., 2013. Chemical insights, explicit chemistry, and yields of secondary organic aerosol from OH radical oxidation of methylglyoxal and glyoxal in the aqueous phase. Atmos. Chem. Phys., 13, 8651-8667.

Loeffler, K.W., Koehler, C.A., Paul, N.M., De Haan, D.O., 2006. Oligomer formation in evaporating aqueous glyoxal and methyl glyoxal solutions. Environ. Sci. Technol. 40, 6318–6323.

McNeill, V.F., Wolfe, G.M., Thornton, J.A., 2007. The oxidation of oleate in submicron aqueous salt aerosols: Evidence of a surface process. J. Phys. Chem. A 111, 1073-1083.

Michaud, V., El Haddad, I., Liu, Y., Sellegri, K., Laj, P., Villani, P., Picard, D., Marchand, N., Monod, A., 2009. In-cloud processes of methacrolein under simulated conditions–Part 3: Hygroscopic and volatility properties of the formed secondary organic aerosol. Atmos. Chem. Phys. 9, 5119-5130.

Millet, D.B., 2005. Atmospheric volatile organic compound measurements during the Pittsburgh Air Quality Study: Results, interpretation, and quantification of primary and secondary contributions. J. Geophys. Res. 110, D07S07.

Munger, J.W., Jacob, D., Daube, B., Horowitz, L., Keene, W., Heikes, B., 1995. Formaldehyde, glyoxal, and methylglyoxal in air and cloudwater at a rural mountain site in central Virginia. J. Geophys. Res. 100, 9325-9325.

Ortiz-Montalvo, D.L., Lim, Y.B., Perri, M.J., Seitzinger, S.P., Turpin, B.J., 2012. Volatility and yield of glycolaldehyde SOA formed through aqueous photochemistry and droplet evaporation. Aerosol Sci. Technol. 46, 1002-1014.

Ortiz-Montalvo, D.L., Häkkinen, S.A., Schwier, A.N., Lim, Y.B., McNeill, V.F., Turpin, B.J., 2014. Ammonium addition (and aerosol pH) has a dramatic impact on the volatility and yield of glyoxal secondary organic aerosol. Environ. Sci. Technol. 48, 255-262.

Paciga, A.L., Riipinen, I., Pandis, S.N., 2014. Effect of Ammonia on the Volatility of Organic Diacids. Environ. Sci. Technol. *48*, 13769-13775.

Pankow, J., Asher, W., 2008. SIMPOL. 1: a simple group contribution method for predicting vapor pressures and enthalpies of vaporization of multifunctional organic compounds. Atmos. Chem. Phys. 8, 2773-2796.

Peng, C., Chan, M.N., Chan, C.K., 2001. The hygroscopic properties of dicarboxylic and multifunctional acids: Measurements and UNIFAC predictions. Environ. Sci. Technol. 35, 4495-4501.

McNeill, V.F., 2015. Aqueous organic chemistry in the atmosphere: Sources and chemical processing of organic aerosols. Environ. Sci. Technol. 49, 1237-1244.

Seinfeld, John H., and Spyros N. Pandis. *Atmospheric chemistry and physics: from air pollution to climate change*. John Wiley Sons, 2012.

Tan, Y., Carlton, A.G., Seitzinger, S.P., Turpin, B.J., 2010. SOA from methylglyoxal in clouds and wet aerosols: Measurement and prediction of key products. Atmos. Environ. 44, 5218-5226.

Tan, Y., Lim, Y.B., Altieri, K.E., Seitzinger, S.P., Turpin, B.J., 2012. Mechanisms leading to oligomers and SOA through aqueous photooxidation: insights from OH radical oxidation of acetic acid and methylglyoxal. Atmos. Chem. Phys. 12, 801-813.

Tsigaridis, K., Kanakidou, M., 2003. Global modelling of secondary organic aerosol in the troposphere: A sensitivity analysis. Atmos. Chem. Phys. 3, 1849-1869.

Turpin, B. J., Lim, H.-J., 2001. Species contributions to PM2.5 mass concentrations: Revisiting common assumptions for estimating organic mass. Aerosol Sci. Technol. 35, 602-610.

U.S. EPA, 2010. Estimation Programs Interface Suite™ for Microsoft® Windows, V4.00. United States Environmental Protection Agency (U.S. EPA), Washington, DC.

Watson, K.M., 1943. Thermodynamics of the liquid state. Ind. Eng. Chem. 35, 398-406.

Weller, C., Tilgner, A., Brauer, P., Herrmann, H., 2014. Modeling the impact of iron-carboxylate photochemistry on radical budget and carboxylate degradation in cloud droplets and particles. Environ. Sci. Technol. 48, 5652-5659.

Yaws, C.L., 2003. Yaws' handbook of thermodynamic and physical properties of chemical compounds. http://wwwknovelcom.

Table Captions

Table 1. VOAG results for MGly + ˙OH precursor/product mixtures: slope (*PM mass / OM mass*$_{(droplet)}$); coefficients of determination (r^2); standard error; effective liquid vapor pressures ($p'_{L,eff.}$); effective enthalpies of vaporization ($\Delta H_{vap,eff.}$).

Table 2. Effective enthalpies of vaporization ($\Delta H_{vap,\ eff.}$) for individual products of MGly + ˙OH, from Clausius-Clapeyron analysis of TPD Aerosol-CIMS data.

Figure Captions

Fig. 1. Ratios of residual PM volume to *OM mass*$_{(droplet)}$ (*PM vol. / OM mass*$_{(droplet)}$) by VOAG from 1 mM solutions of oxalic acid, ammonium oxalate, pyruvic acid, and sodium pyruvate; mixtures of 1 mM oxalic acid + ammonium hydroxide (Amm. OH) and 1 mM pyruvic acid + ammonium hydroxide (pH ≈ 7) to form ammonium oxalate (Amm. Oxalate) and ammonium pyruvate, respectively. Liquid vapor pressure ($p°_L$) estimates for acids from SIMPOL group contribution (Pankow and Asher, 2008) and for organic salts (sub-cooled $p°_L$) using EPA-EPI Suite™ (U.S. EPA 2010).

Fig. 2. (a) Batch and **(b)** Continuously Stirred-Tank Reactor (CSTR) model results for aqueous photooxidation of 5 µM methylglyoxal (MGly) with 10^{-12} M ˙OH. Methylglyoxal (black), pyruvic acid (pink), acetic acid (green), oxalic acid (orange), formaldehyde (blue). Pie charts provide droplet composition (molar fraction %) at 10 and 30 min. Background shading highlights cloud droplet lifetimes of 10-30 min (Ervens and Volkamer, 2010; Desboeufs et al., 2003).

Fig. 3. Residual particle mass (*PM mass*) and *OM mass*$_{(droplet)}$ formed from VOAG droplet evaporation experiments (12±3% RH and 24.1±0.4ºC). *OM mass*$_{(droplet)}$ is the mass of organic matter in the initial droplet before evaporation. Shown are organic acid standard solutions (dashed light-colored lines): acetic, oxalic, succinic, glutaric, tartaric acid, and mimic sample solutions (solid dark-colored lines): Batch 30 min pH 3; CSTR 10 min pH 3; CSTR 10 min pH 7. Inset: sigmoidal regression of *PM mass / OM mass* vs. *log* p^o_L of standards (black squares with solid line). Inset illustrates how $p'_{L,eff}$ of mimic samples is determined from measured *PM mass / OM mass*$_{(droplet)}$: CSTR 10 min mimic pH 7 (inset red dashed line), Batch 30 min pH 3 (inset blue dashed line), CSTR 10 min pH 3 (inset dark grey dashed line). Table 1 provides estimated effective vapor pressures and enthalpies of vaporization.

528 **Table 1.** VOAG results for MGly + •OH precursor/product mixtures: slope (*PM mass / OM mass*$_{(droplet)}$), coefficients of determination (r^2), standard
529 error; effective liquid vapor pressures ($p'_{L,eff.}$); effective enthalpies of vaporization ($\Delta H_{vap,eff.}$).
530

Mimic Sample	**pH**	**Density (g/mL)**	**Slope** [a]	***Standard Error***	r^2	$p'_{L,eff.}$ [b] **(atm)**	$\Delta H_{vap,eff.}$ [c] **(kJ/mol)**	**Theoretical** $\Delta H_{vap,mix}$ [d] **(kJ/mol)**
Batch 30 min	3	1.2[e]	0.17	0.04	69%	$(4\pm4) \times 10^{-7}$	68 ± 2	44
CSTR 10 min	3	1.1[e]	0.10	0.02	74%	$(6\pm6) \times 10^{-7}$	67 ± 2	42
	7	1.1[f]	0.27	0.05	93%	$(3\pm2) \times 10^{-7}$	69 ± 2	42

531
532

[a] Slopes (in units of g/g) from Fig. 3 corrected by the effect of retained water (33% upper-bound estimate) on the density used to calculate *PM mass*. Slopes for organic acid standards are provided in Ortiz-Montalvo et al. (2012). [b] Effective liquid vapor pressure estimates (at 298.15 K) using a sigmoidal regression provided in Ortiz-Montalvo et al. (2012), which was confined by estimates of vapor pressure of pure compounds using SIMPOL group contribution method ± error propagation (incorporates uncertainty in Pankow and Asher (2008) estimates, standard error of slope, and standard error in the coefficients of the sigmoidal regression). [c] Effective enthalpy of vaporization estimates (at normal boiling point) using a sigmoidal regression provided in Ortiz-Montalvo et al. (2012), which was defined by estimates of enthalpy of vaporization of pure compounds at normal boiling point ± error propagation (incorporates uncertainty in Joback and Reid (1987), standard error of slope, and standard error in the coefficients of the sigmoidal regression). [d] Molar weighted theoretical enthalpies of vaporization of product mixtures calculated following Chickos et al. (2005) approach, as $\Delta H_{vap,mix} = \sum_i n_i \times \Delta H_{vap,i}$ where n_i is the molar fraction of species *i* (from Fig. 2) and $\Delta H_{vap,i}$ is the theoretical enthalpy of vaporization of species *i* (reported in Table 2). [e] Concentration-weighted density (Turpin and Lim, 2001) ± 0.1 (error propagation accounting for the uncertainty in the concentrations). [f] Assumed the same density as for CSTR 10 min pH 3. Sensitivity analysis showed that with varying density (from 0.8 to 1.5 g/mL), the enthalpy of vaporization and vapor pressure were essentially unchanged (68-69 kJ/mol and (3-2) × 10^{-7} atm, respectively).

Table 2. Effective enthalpies of vaporization ($\Delta H_{vap,\,eff.}$) for individual products of MGly + •OH, from Clausius-Clapeyron analysis of TPD Aerosol-CIMS data.

		$\Delta H_{vap,\,eff.}$ [a] (kJ/mol)		
Organic Species	**Theoretical ΔH_{vap} (kJ/mol)**	**Batch 30 min**	**CSTR 10 min**	
		pH 3.8	**pH 3.7**	**pH 4.6**
Pyruvic acid (*m/z 215*)	48 – 52 [b]	$6^{\pm 2}$	$19^{\pm 9}$	$5^{\pm 3}$
Oxalic acid / Methylglyoxal (*m/z 217*)	90 – 97 [b] / 30 – 35 [c]	$34^{\pm 2}$	$31^{\pm 5}$	$32^{\pm 3}$

a – effective enthalpy of vaporization at 25-116ºC; average values weighted by the standard deviations (n=2) ± one standard deviation (in superscript).

b – average theoretical enthalpy of vaporization at 25-116ºC taken from Yaws (2003).

c –average theoretical enthalpy of vaporization at 25ºC taken from SPARC online calculator (Hilal et al., 2003), and adjusted to the temperature range used in the TPD Aerosol-CIMS experiments (25-116ºC) by using Watson's equation (Watson 1943).

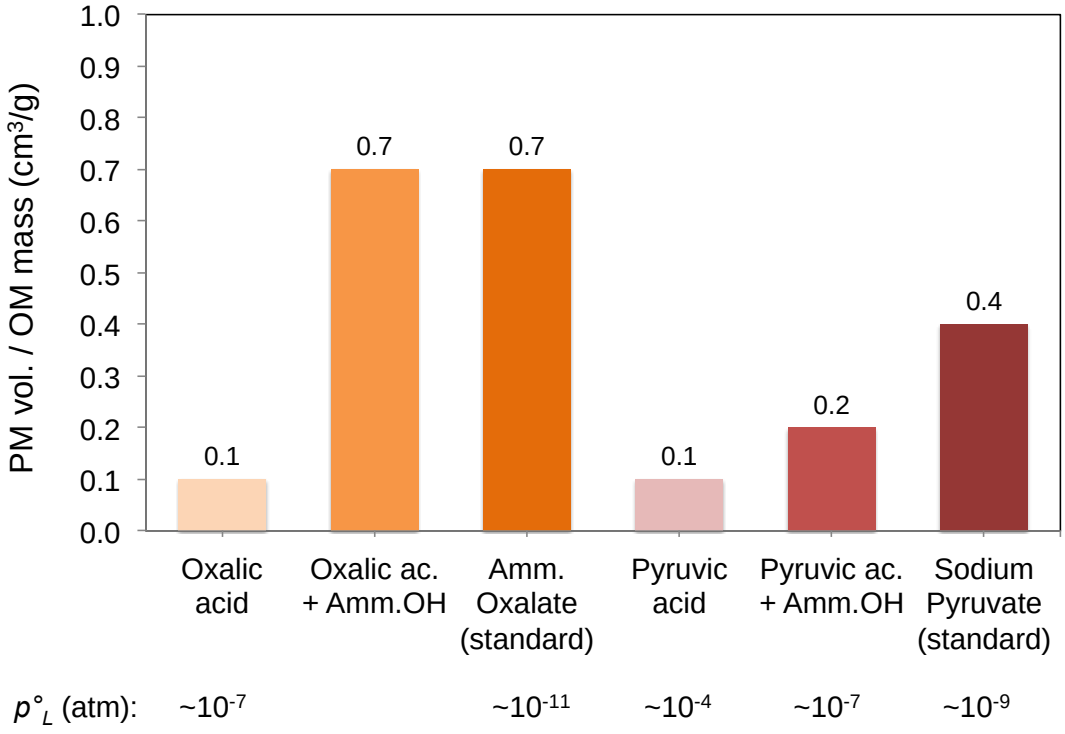

548
549

550 **Fig. 1.** Ratios of residual PM volume to *OM mass*$_{(droplet)}$ (*PM vol. / OM mass*$_{(droplet)}$) by VOAG from
551 1 mM solutions of oxalic acid, ammonium oxalate, pyruvic acid, and sodium pyruvate; mixtures of 1
552 mM oxalic acid + ammonium hydroxide (Amm. OH) and 1 mM pyruvic acid + ammonium
553 hydroxide (pH ≈ 7) to form ammonium oxalate (Amm. Oxalate) and ammonium pyruvate,
554 respectively. Liquid vapor pressure ($p°_L$) estimates for acids from SIMPOL group contribution
555 (Pankow and Asher, 2008) and for organic salts (sub-cooled $p°_L$) using EPA-EPI Suite™ (U.S. EPA
556 2010).

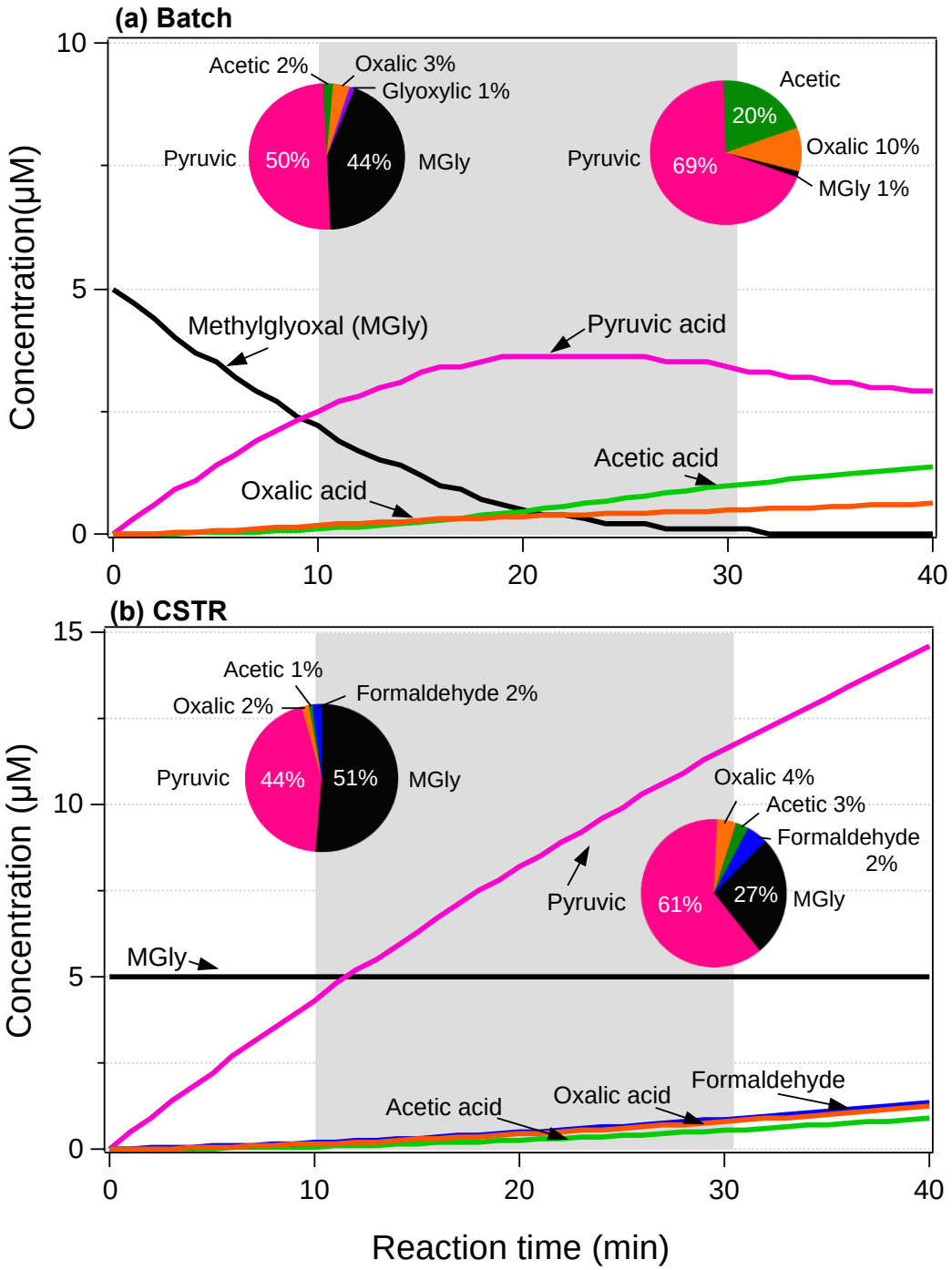

Fig. 2. (a) Batch and **(b)** Continuously Stirred-Tank Reactor (CSTR) model results for aqueous photooxidation of 5 μM methylglyoxal (MGly) with 10^{-12} M ˙OH. Methylglyoxal (black), pyruvic acid (pink), acetic acid (green), oxalic acid (orange), formaldehyde (blue). Pie charts provide droplet composition (molar fraction %) at 10 and 30 min. Background shading highlights cloud droplet lifetimes of 10-30 min (Ervens and Volkamer, 2010; Desboeufs et al., 2003).

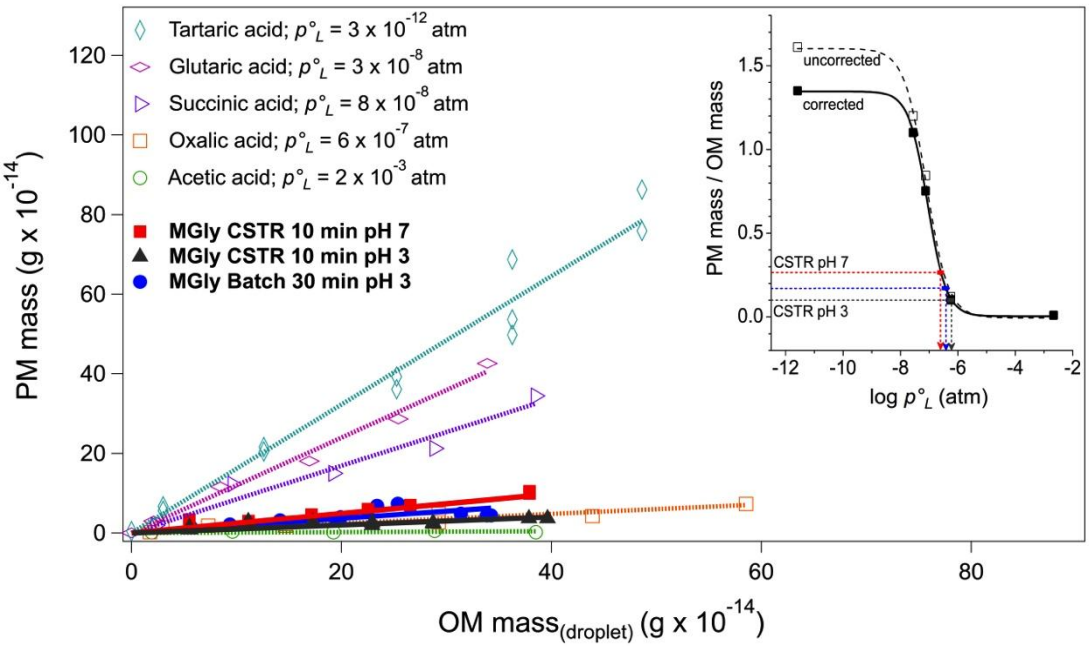

Fig. 3. Residual particle mass (*PM mass*) and *OM mass*$_{(droplet)}$ formed from VOAG droplet evaporation experiments (12±3% RH and 24.1±0.4ºC). *OM mass*$_{(droplet)}$ is the mass of organic matter in the initial droplet before evaporation. Shown are organic acid standard solutions (dashed light-colored lines): acetic, oxalic, succinic, glutaric, tartaric acid, and mimic sample solutions (solid dark-colored lines): Batch 30 min pH 3; CSTR 10 min pH 3; CSTR 10 min pH 7. Inset: sigmoidal regression of *PM mass / OM mass* vs. *log* p^{o}_{L} of standards (black squares with solid line). Inset illustrates how $p'_{L,eff}$ of mimic samples is determined from measured *PM mass / OM mass*$_{(droplet)}$: CSTR 10 min mimic pH 7 (inset red dashed line), Batch 30 min pH 3 (inset blue dashed line), CSTR 10 min pH 3 (inset dark grey dashed line). Table 1 provides estimated effective vapor pressures and enthalpies of vaporization.